



River Breezes for Pollutant Dispersion in GoAmazon2014/5

Adan S. S. Medeiros^{1,2}, Igor O. Ribeiro¹, Marcos V. B. Morais⁴, Rita V. Andreoli³, Jorge A. Martins⁵, Leila D. Martins⁶, Carla E. Batista¹, Patrícia C. Guimarães¹, Scot T. Martin^{*,7},
Rodrigo A. F. Souza^{*,3}.

¹ Post-graduate Program in Climate and Environment, CLIAMB, INPA/UEA, Av. André Araújo, 2936, 69060001, Manaus, Amazonas, Brazil

² Amazonas State University, Center of Superior Studies of Tefé, R. Brasília, 2127, 69470-000, Tefé, Amazonas, Brazil

³ Amazonas State University, Superior School of Technology, Av Darcy Vargas, 1200, 69065020, Manaus, Amazonas, Brazil

⁴ Post-graduate Program in Environmental Engineering, Federal University of Technology, Av dos Pioneiros, 3131, 86047-125, Londrina, Paraná, Brazil;

⁵ Department of Physics, Federal University of Technology, Av dos Pioneiros, 3131, 86047-125, Londrina, Paraná, Brazil;

⁶ Department of Chemistry, Federal University of Technology, Av dos Pioneiros, 3131, 86047-125, Londrina, Paraná, Brazil;

⁷ School of Engineering and Applied Sciences, Harvard University, 02138, Cambridge, Massachusetts, USA

E-mail: scot_martin@harvard.edu, souzaraf@gmail.com

*To Whom Correspondence Should be addressed



1 Abstract

2 The effect of river breezes on pollutant plume dispersion or canalization in the central
3 Amazon was evaluated. A pollution plume changes atmospheric composition downwind of
4 Manaus, a city of 2 million people positioned at the confluence between two wide rivers. Herein,
5 to evaluate the effects of river breezes, two cases were modeled at the mesoscale for March
6 2014. The first case, “with rivers” (wR), simulated the transport and chemistry of the Manaus
7 pollution plume as the rivers were in reality. The second case, “without rivers” (woR), carried
8 out simulations for which all rivers and floodable areas were replaced by forest. The three main
9 conclusions are as follows: (1) Between the two cases, alterations in wind speeds were maximum
10 at local noon, and river breezes influenced horizontal wind fields from surface up to 150 m in
11 altitude, suggesting a capping height of 150 m on most days for the influence of river breezes on
12 pollutant concentrations. In agreement with this modeling result, data sets collected at 500 m by
13 aircraft flights showed no apparent influence of the underlying rivers on plume dispersion. The
14 flights traversed the plume downwind of Manaus during the *Observations and Modeling of the*
15 *Green Ocean Amazon (GoAmazon2014/5) Experiment*. (2) Between the wR and woR cases,
16 changes to downwind concentrations of O₃, NO_x, and CO pollutants were < 6% as a monthly
17 average at the supersite “T3” of GoAmazon2014/5, which was 70 km downwind of Manaus and
18 located between the two main rivers. As single events at T3, maximum one-hour concentration
19 differences were 39 ppb for O₃, 5 ppb for NO_x, and 26 ppb for CO. (3) For a focus on the surface
20 layer of the rivers (0 to 150 m in height), river breezes increased the monthly average O₃, NO_x,
21 and CO surface concentrations by 25%, 25%, and <5%, respectively. In addition, strong
22 canalization occurred 5% of the time based on a difference of 10 ppb in the surface
23 concentrations of at least two of O₃, NO_x, and CO between the wR and woR cases. In
24 conclusion, although pollutants dispersed by river breezes could at times be a strong effect on
25 observed pollutant concentrations in the surface river boundary layer, overall most pollution was
26 transported at heights well above the effects of the river breezes and moved downwind along the
27 trajectories of the dominant trade winds.



28 1. Introduction

29 Amazonia represents the single largest hydrographic basin of water volume on Earth
30 (Sioli, 1984). Land coverage by rivers constitutes 5% of the total 7 million square kilometers of
31 the Amazon basin during dry season, while in the wet season the rivers increase in horizontal
32 extent by flooding, reaching a surface coverage of 11% of Amazonia (Hess et al., 2015). An
33 important confluence of wide rivers occurs nearby Manaus, a city of more than 2 million people
34 located at {3.0° S, 60.0° W} in the central Amazon (Figure 1). The Rio Negro (“Black River”)
35 flows from the northwest to join the Amazon River, known in Brazil as the Rio Solimões to the
36 west of Manaus and the Rio Amazonas to the east of Manaus. River width around Manaus varies
37 from 2 km in narrow sections to 20 km in broader sections.

38 Wide rivers such as these can induce important atmospheric processes, among which are
39 river breezes (Oliveira and Fitzjarrald, 1993; Dias et al., 2004; dos Santos et al., 2014). River
40 breezes arise from the unequal heating of land and water bodies. In the morning, land heats faster
41 than water, inducing an ascendancy of air over the land and a corresponding subsidence over the
42 river. In this way, surface winds go from the river toward the land. At an altitude of a few
43 hundred meters, the circulation cell is closed, and the winds go from the land to the river, with
44 subsidence over the central portion of the river. The height of the cell depends on the thermal
45 characteristics of the circulation. At night, the opposite behavior occurs (i.e., the cell reverses)
46 because the river cools more rapidly than land.

47 These river breeze circulations at day and night can be important for the local weather
48 and pollutant dispersion. For instance, during times of weak trade winds Dias et al. (2004) found
49 that river breeze circulation explained the occurrence of clouds on the eastern bank yet an



50 absence on the western bank at the confluence between the Amazon and Tapajós rivers, about
51 600 km to the east of Manaus.

52 Oliveira and Fitzjarrald (1993, 1994) studied the river breezes in the Manaus region
53 during the Amazon Boundary Layer Experiments (ABLE) (Garstang et al., 1990; Harriss et al.,
54 1990). Based on observations of the meridional component of wind speed, the river breezes were
55 reported as more intense during the dry season than in the wet season, as explained by greater
56 contrast between river and land temperatures given the greater average insolation of the dry
57 season. Simulations further suggested that the river breeze induced by the Rio Negro
58 significantly affected the surrounding daytime surface winds to a distance of 20 km from the
59 rivers (Oliveira and Fitzjarrald, 1994). The modeled distance was further than initially expected
60 based on earlier modeling studies, and the key difference appeared to be an improved
61 representation of the planetary boundary layer (PBL) in the model.

62 As part of the Large-Scale Biosphere-Atmosphere Experiment in Amazonia-Cooperative
63 LBA Airborne Regional Experiment-2001 (LBA-CLAIRE-2001), Trebs et al. (2012) traveled by
64 boat to four locations on the Rio Negro and one on the Solimões River. Daily reversals in surface
65 winds were attributed to river breezes. Measurements were made of NO, NO₂, and O₃ surface
66 concentrations, and pollution was identified at surface river locations from 10 to 150 km
67 downwind from Manaus. On at least one day, a reversal in wind direction caused by the
68 afternoon influence of the river breeze was associated with a shift in concentrations
69 representative of background and polluted conditions. Manaus pollution directed by the river
70 breezes appeared to be the explanation. The important data sets of this study were, however,
71 overall sparse (i.e., 8 days of July 2001; Manaus population of 1.2 million at that time), and the
72 recommendation by the authors was therefore to implement long-term monitoring stations



73 downwind Manaus and to apply mesoscale modeling to better understand river breeze effects on
74 the dispersion of the Manaus pollution plume.

75 In 2014 and 2015, the Observations and Modeling of the Green Ocean Amazon
76 (GoAmazon2014/5) Experiment was carried out to study the effects of pollutant outflow from
77 Manaus on atmospheric chemistry, regional climate, and terrestrial ecosystems of an otherwise
78 typically clean background environment (Martin et al., 2016). Under fair-weather conditions, the
79 pollution plume was carried westward by equatorial trade winds (Kuhn et al., 2010; Martin et al.,
80 2017). The GoAmazon2014/5 terrestrial supersite, called “T3”, was 70 km to the west of Manaus
81 (Figure 1).

82 An important question for the GoAmazon2014/5 experiment was to what extent river
83 breezes might disperse or canalize Manaus pollution, thereby possibly influencing the
84 interpretation of data sets collected at the T3 supersite. For a limiting case of full river
85 canalization, no pollution would reach the T3 site. For an opposite limiting case of weak or no
86 river breeze effects, all pollution would follow the stable trade winds when fair-weather
87 conditions prevailed, and air parcels sampled at the T3 site would be interpreted in a fully
88 Lagrangian framework downwind of the Manaus source region. Between these limiting cases,
89 partial dispersion of the Manaus pollution plume would be possible. In the context of these
90 possibilities and in light of the work of Oliveira and Fitzjarrald (1993, 1994) and Trebs et al.
91 (2012), the study herein presents an analysis of how the rivers around Manaus affect downwind
92 pollutant dispersion or canalization. The analysis uses mesoscale WRF-Chem modeling and
93 GoAmazon2014/5 data sets.



94 **2. Simulations**

95 2.1 *Model Description*

96 The *Weather Research and Forecast model coupled with Chemistry* (WRF-Chem) is
97 described by Grell et al. (2005). Version 3.6.1 was used for the present study. A two-domain
98 configuration was used (Medeiros et al., 2017). The inner domain represented an area of 302 km
99 × 232 km, had a horizontal resolution of 2 km × 2 km, and had 38 vertical layers from ground to
100 160 hPa. The outside boundaries of the inner domain were forced by data from an outer domain.
101 The outer domain represented an area of 1050 km × 800 km, had a resolution of 10 km × 10 km,
102 and had 38 vertical layers from ground to 160 hPa. Both domains were centered on {2.908° S,
103 60.319° W}. The meteorology of the outside boundary of the outer domain was forced by the
104 *Climate Forecast System Reanalysis* (CFSv2) product of the National Center for Environment
105 Prediction (NCEP) at a temporal resolution of 6 h and a spatial resolution of 0.5° (Saha et al.,
106 2011). The inputs of surface temperature were also considered based on CFSv2 product. The
107 chemical composition of the outside boundary of the outer domain was forced by the Model *for*
108 *Ozone and Related chemical Tracers* (MOZART-4) (Emmons et al., 2010).

109 Data of the Moderate Resolution Imaging Spectroradiometer (MODIS) satellite at a
110 resolution of 500 m were used for land cover (Channan et al., 2014). These data were used as
111 obtained for the case of “with rivers” (wR). For the case of “without rivers” (woR), the rivers
112 and main flooded areas of MODIS land cover were replaced by forest in the pre-processor of the
113 WRF-Chem model.

114 The physics parametrizations used in the simulations were described previously (Ying et
115 al., 2009; Misenis and Zhang, 2010; Gupta and Mohan, 2015), including for the study region in
116 the central Amazon (Medeiros et al., 2017). The parametrizations treated the physics of the



117 surface layer (Grell et al., 1994), the land surface (Chen et al., 1997), the boundary layer (Hong
118 et al., 2006), shortwave radiation (Chou and Suarez, 1999), longwave radiation (Mlawer et al.,
119 1997), cloud microphysics (Lin et al., 1983), and cumulus clouds (Grell and Freitas, 2014). At
120 Figure S1, the comparison between observed and simulated temperature, relative humidity and
121 wind speed at “T3” supersite show that the simulations performed herein represent the diurnal
122 cycle of these variables.

123 For chemical parametrizations, the *Model of Emissions of Gases and Aerosols from*
124 *Nature* (MEGAN, version 2.1) (Guenther et al., 2012) was used for biogenic emissions.
125 Anthropogenic emissions from transport, power, and industry for Manaus in 2014 were based on
126 the emission inventory of Medeiros et al. (2017). The *Regional Acid Deposition Model*
127 (RADM2) was used to simulate gas-phase chemistry (Chang et al., 1989).

128 2.2 Model Runs

129 Simulations of the wR and woR cases were carried out for all days in March 2014. Other
130 characteristics between the two simulations remained the same. This approach aimed to isolate
131 the river breeze effects on the transport of pollutants downwind of Manaus. For time zero, the
132 inner and outer domains were both initialized to CFSv2 and MOZART-4. A spin-up time of 24 h
133 was used, which was sufficient to fully replace the air of the inner domain. After the spin-up
134 period, simulations in lots of 72 h were performed for March 2014 as a balance between
135 conserving computing resources and avoiding excessive numerical drift (Medeiros et al., 2017).

136 3. Data Sets

137 Data sets were collected during the first intensive operating period (IOP1) of the
138 GoAmazon2014/5 project by instrumentation of the G-159 Gulfstream I (G-1) of the ARM
139 Aerial Facility (AAF) of the USA Department of Energy (Schmid et al., 2014; Martin et al.,



140 2017). Concentrations of O₃ (Thermo Scientific Model 49i), NO_x (airborne NO_x analyzer, Air
141 Quality Devices), and CO (Los Gatos 23r) were measured. The aircraft performed 16 flights
142 during IOP1. Data sets of two flights (March 14 and 21) were chosen for analysis herein based
143 on flight tracks over both river and land while cutting across the Manaus pollution plume at an
144 altitude of approximately 500 m. There were no flights at lower altitude.

145 **4. Results and Discussion**

146 *4.1 Height of River Breeze Circulation Cell*

147 The effect of river breezes on horizontal wind speeds was evaluated. As monthly means,
148 the left column of Figure 2 presents the wR case, and the right column shows the differences
149 between the wR and woR cases. The rows represent plots at surface, 100-m altitude, and 500-m
150 altitude. Comparison between columns shows that the river breezes significantly affected mean
151 surface wind speeds but that the effects decreased with altitude.

152 The change of horizontal wind speeds with altitude is presented in detail in Figure 3
153 through height cross sections along points A, B, and C above the Rio Negro nearby Manaus (cf.
154 Figure 1). Panels in Figure 3 show wind speed differences between the wR and woR cases for all
155 times as well as for 00:00, 06:00, 12:00, and 18:00 (local time). In the absence of solar radiation
156 (i.e., at 00:00 and 18:00 local), the differences in horizontal wind speeds were relatively small.
157 The strongest differences were at noon corresponding to maximum daily solar irradiance, as
158 expected, because of the largest thermal gradients between land and river at these times (Oliveira
159 and Fitzjarrald, 1993, 1994; Dias et al., 2004; Fitzjarrald et al., 2008; de Souza and dos Santos
160 Alvalá, 2014; dos Santos et al., 2014; de Souza et al., 2016). The river breeze effect was
161 confined to less than 150 m, as shown in the monthly average plot of Figure 3. Across individual
162 days, the maximum and minimum heights for significant noontime river breeze effects were 300



163 and 60 m, respectively (results not shown). Overall, the results of Figures 2 and 3 lead to the
164 conclusion that the river breeze effect on wind speeds was confined on most days to below 150
165 m in altitude, even under high noontime solar irradiance.

166 For comparison, aircraft data sets of O₃, NO_x, and CO concentrations from 500-m altitude
167 are plotted in Figure 4 (Martin et al., 2017). Carbon monoxide was mostly inert on the time
168 scales of the simulations, oxides of nitrogen were significantly lost during downwind transport,
169 and ozone was a secondary pollutant rapidly produced within Manaus and over the nearby rivers,
170 quickly reaching steady-state concentrations (Medeiros et al., 2017; Rafee et al., 2017). The
171 panels of the left column of Figure 4 show that the flight paths intercepted the Manaus pollution
172 plume in the planetary boundary layer on March 14 from 10:20 to 11:20 (local time; UTC - 4 h).
173 The panels of the right column show that interception took place on March 21 from 13:00 to
174 14:00. Below each map, concentrations along the flight tracks are plotted, and the red shading
175 represents times that the aircraft was over a river. The results show that there was no obvious
176 influence of river breezes on the dispersion of the Manaus pollutant plume at 500 m. Although
177 Figure 4 shows only two flights, which were selected for substantial data coverage over both
178 river and land during a single flight, all 16 flights from March 2014 were investigated, and a
179 strong river breeze effect was not apparent in any of them (analysis not shown). The aircraft data
180 sets thus corroborate the tendencies represented in Figures 2 and 3 that the effects of rivers
181 presence on plume dispersion are confined to the surface boundary layer over the rivers,
182 typically below 150 m.

183 4.2 *Effects of River Breezes on Downwind Concentrations*

184 The “T3” GoAmazon2014/5 terrestrial supersite was located at {-3.2133 N, -60.5987 E},
185 approximately 70 km to the west of Manaus and in the dominant direction of prevailing trade



186 winds that passed through Manaus (Figure 1). The panels in the top row of Figures 5, 6, and 7
187 show O₃, NO_x, and CO concentrations, respectively, at the T3 location for the wR case as the
188 blue line, the woR case as the red line, and their difference as the black line. The pollutant
189 concentrations did not change greatly in the presence or absence of the rivers. Quantitatively, the
190 perturbations caused by the presence of the rivers on the O₃, NO_x, and CO concentrations were
191 less than 6%. Maximum one-hour concentration differences were 39 ppb for O₃, 5 ppb for NO_x,
192 and 26 ppb for CO across the month. The overall implication is that the effects of the trade winds
193 on transport largely dominated over the influence of river breezes in this region when
194 considering the larger part of Manaus pollutant outflow, in agreement with the modeling and
195 observational results of section 4.1.

196 4.3 Surface River Concentrations

197 Two locations “R1” and “R2” were chosen to evaluate pollutant dispersion and
198 canalization in the river surface layer (0 to 150 m). Based on the prevailing trade winds location
199 R1 at {-3.0699 N, -60.2199 E} consistently intercepted the urban outflow (Figure 1). By
200 comparison, location R2 at {-2.9800 N, -60.4901 E} was nominally outside of the trajectories of
201 the trade winds that passed over and then downwind of Manaus. For the analysis, the simulated
202 pollutant concentrations at R2 were compared to those at R1 in the wR and woR cases to test the
203 extent of river canalization of the plume, meaning transport of air parcels along the river rather
204 than in the prevailing direction of the synoptic-scale trade winds.

205 The time series of the simulated O₃, NO_x, and CO concentrations at the R1 and R2
206 locations are plotted in Figures 5, 6, and 7. Blue lines show the wR case, red lines show the woR
207 case, and black lines represent their difference. At R1, the differences of (wR - woR) were
208 significant, in particular for concentrations of O₃ (+28.4%) and NO_x (+26.0%) (Table 1, monthly



209 means). Strong differences were also simulated at R2 for O_3 (+25.5%) and NO_x (+25.6%). The
210 river breezes thus shifted the surface level dispersion pattern of the Manaus plume. At both sites,
211 the differences were smaller (< 5%) for CO concentrations because regional background
212 concentrations exceeded the Manaus contribution. Absolute changes (\pm ppb) for four time
213 periods across the day are listed in Table S1 of the Supplementary Material. The difference
214 between the wR and woR cases exceeded 10 ppb at R2, which can be called strong canalization,
215 for at least two pollutants at 5% frequency for March 2014.

216 An example of strong canalization occurred for the simulation on March 2 at 13:00 (local
217 time). The three columns of Figure 8 show the wR case, the woR case, and their difference, all at
218 surface altitude. The three rows show results for O_3 , NO_x , and CO. For the wR case, a small
219 portion of the pollution plume traversed the course of Rio Negro to the northwest, following the
220 local wind field. A boat collecting surface samples would report increases of O_3 by 20 ppb and of
221 CO by 10 ppb. Overall, comparison of the wR and woR case shows that the simulated plume was
222 tighter with less transverse spreading in the absence of rivers. In both the wR and woR cases,
223 most pollution followed the predominant direction of the trade winds, and the effects of river
224 canalization on diverting the plume were small by comparison.

225 In summary, this study evaluated the effects of river breezes on pollutant plume
226 dispersion or canalization in the central Amazon. The simulations showed that the horizontal
227 monthly mean wind speeds were significantly altered by river breezes to altitudes of 75 m as
228 monthly 24-h means and to 150 m for monthly averages across the maximum noontime solar
229 radiation. The strongest effects of river breezes on pollutant dispersion were thus from 0 to 150
230 m above the river surface. Aircraft data confirmed the absence of observable effects of river
231 breezes on plume dispersion at flight level (500 m). Overall, the perturbation on pollutant



232 concentrations downwind of Manaus at “T3” GoAmazon2014/5 supersite was modeled as below
233 6%, consistent with pollutant transport mostly above 150 m. At river surface level, the monthly
234 average O₃, NO_x, and CO surface concentrations increased by 25%, 25%, and <5%, respectively.
235 Differences in surface river concentrations exceeded 10 ppb for at least two pollutants at a
236 frequency of 5% for March 2014. The overall conclusion is that the Manaus pollution plume
237 dispersion could at times be partially canalized leading to significant changes of surface river
238 concentrations even as most pollution passed overhead of the river circulation cell and
239 dominantly followed trajectories along the prevailing overhead trade winds.

Acknowledgments

We acknowledge support from the Central Office of the Large-Scale Biosphere-Atmosphere Experiment in Amazonia (LBA), the National Institute of Amazonian Research (INPA), the Amazonas State University (UEA), the Brazilian Innovation Agency (FINEP), and the Atmospheric System Research (ASR) program of the Office of Biological and Environmental Research, Office of Science, United States Department of Energy (DOE) (grant DE-SC0011115). A. Medeiros thanks the Brazilian Federal Agency for Support and Evaluation of Graduate Education (CAPES) for the grant scholarship, linked to the doctoral program in Climate and Environment (CLIAMB). Funding was received under grant 062.00568/2014 of the Amazonas State Research Foundation (FAPEAM). A FAPEAM grant of a Senior International Visiting Researcher is also acknowledged. The work was conducted under scientific licenses 001030/2012-4 and 400063/2014-0 of the Brazilian National Council for Scientific and Technological Development (CNPq).



References

- Chang, J., Middleton, P., Stockwell, W., Binkowski, F., and Byun, D.: The regional acid deposition model and engineering model, State-of-Science/Technology, National Acid Precipitation Assessment Program, 1989.
- Channan, S., Collins, K., and Emanuel, W.: Global mosaics of the standard MODIS land cover type data, University of Maryland and the Pacific Northwest National Laboratory, College Park, Maryland, USA, 30, 2014.
- Chen, F., Janjić, Z., and Mitchell, K.: Impact of Atmospheric Surface-layer Parameterizations in the new Land-surface Scheme of the NCEP Mesoscale Eta Model, *Bound.-Layer Meteorol.*, 85, 391-421, 10.1023/a:1000531001463, 1997.
- Chou, M.-D., and Suarez, M. J.: A solar radiation parameterization for atmospheric studies, NASA Tech. Memo, 104606, 40, 1999.
- de Souza, D. O., and dos Santos Alvalá, R. C.: Observational evidence of the urban heat island of Manaus City, Brazil, *Meteorological Applications*, 21, 186-193, 10.1002/met.1340, 2014.
- de Souza, D. O., dos Santos Alvalá, R. C., and do Nascimento, M. G.: Urbanization effects on the microclimate of Manaus: A modeling study, *Atmospheric Research*, 167, 237-248, 2016.
- Dias, M. S., Dias, P. S., Longo, M., Fitzjarrald, D. R., and Denning, A. S.: River breeze circulation in eastern Amazonia: observations and modelling results, *Theor. Appl. Climatol.*, 78, 111-121, 10.1007/s00704-004-0047-6, 2004.
- dos Santos, M. J., Silva Dias, M. A. F., and Freitas, E. D.: Influence of local circulations on wind, moisture, and precipitation close to Manaus City, Amazon Region, Brazil, *Journal of Geophysical Research: Atmospheres*, 119, 13,233-213,249, 10.1002/2014jd021969, 2014.
- Emmons, L., Walters, S., Hess, P., Lamarque, J.-F., Pfister, G., Fillmore, D., Granier, C., Guenther, A., Kinnison, D., and Laepple, T.: Description and evaluation of the Model for Ozone and Related chemical Tracers, version 4 (MOZART-4), *Geosci. Model Dev.*, 3, 43-67, 10.5194/gmd-3-43-2010, 2010.



- Fitzjarrald, D. R., Sakai, R. K., Moraes, O. L., Cosme de Oliveira, R., Acevedo, O. C., Czikowsky, M. J., and Beldini, T.: Spatial and temporal rainfall variability near the Amazon-Tapajós confluence, *J. Geophys. Res.*, 113, n. G1, 10.1029/2007JG000596, 2008.
- Garstang, M., Greco, S., Scala, J., Swap, R., Ulanski, S., Fitzjarrald, D., Martin, D., Browell, E., Shipman, M., and Connors, V.: The Amazon boundary-layer experiment (ABLE 2B): A meteorological perspective, *Bull. Am. Meteorol. Soc.*, 71, 19-32, 10.1175/1520-0477(1990)071<0019:TABLEA>2.0.CO;2, 1990.
- Grell, G. A., Devenyi, J., Dudhia, J., and Stauffer, D. R.: A description of the fifth-generation Penn State/NCAR mesoscale model (MM5). NCAR Tech. Note NCAR/TN-398STR., 1994.
- Grell, G. A., Peckham, S. E., Schmitz, R., McKeen, S. A., Frost, G., Skamarock, W. C., and Eder, B.: Fully coupled “online” chemistry within the WRF model, *Atmos. Environ.*, 39, 6957-6975, 10.1016/j.atmosenv.2005.04.027, 2005.
- Grell, G. A., and Freitas, S. R.: A scale and aerosol aware stochastic convective parameterization for weather and air quality modeling, *Atmos. Chem. Phys.*, 14, 5233-5250, 10.5194/acp-14-5233-2014, 2014.
- Guenther, A. B., Jiang, X., Heald, C. L., Sakulyanontvittaya, T., Duhl, T., Emmons, L. K., and Wang, X.: The Model of Emissions of Gases and Aerosols from Nature version 2.1 (MEGAN2.1): an extended and updated framework for modeling biogenic emissions, *Geosci. Model Dev.*, 5, 1471-1492, 10.5194/gmd-5-1471-2012, 2012.
- Gupta, M., and Mohan, M.: Validation of WRF/Chem model and sensitivity of chemical mechanisms to ozone simulation over megacity Delhi, *Atmos. Environ.*, 122, 220-229, 10.1016/j.atmosenv.2015.09.039, 2015.
- Harriss, R., Garstang, M., Wofsy, S., Beck, S., Bendura, R., Coelho, J., Drewry, J., Hoell, J., Matson, P., and McNeal, R. J.: The Amazon boundary layer experiment: wet season 1987, *J. Geophys. Res.*, 95, n. D10, 16721-16736, 10.1029/JD095iD10p16721, 1990.
- Hong, S.-Y., Noh, Y., and Dudhia, J.: A new vertical diffusion package with an explicit treatment of entrainment processes, *Mon. Weather Rev.*, 134, 2318-2341, 10.1175/MWR3199.1, 2006.



- Kuhn, U., Ganzeveld, L., Thielmann, A., Dindorf, T., Schebeske, G., Welling, M., Sciare, J., Roberts, G., Meixner, F. X., Kesselmeier, J., Lelieveld, J., Kolle, O., Ciccioli, P., Lloyd, J., Trentmann, J., Artaxo, P., and Andreae, M. O.: Impact of Manaus City on the Amazon Green Ocean atmosphere: ozone production, precursor sensitivity and aerosol load, *Atmos. Chem. Phys.*, 10, 9251-9282, [10.5194/acp-10-9251-2010](https://doi.org/10.5194/acp-10-9251-2010), 2010.
- Lin, Y.-L., Farley, R. D., and Orville, H. D.: Bulk parameterization of the snow field in a cloud model, *J. Clim. Appl. Meteorol.*, 22, 1065-1092, [10.1175/1520-0450\(1983\)022<1065:BPOTSF>2.0.CO;2](https://doi.org/10.1175/1520-0450(1983)022<1065:BPOTSF>2.0.CO;2), 1983.
- Martin, S. T., Artaxo, P., Machado, L. A. T., Manzi, A. O., Souza, R. A. F., Schumacher, C., Wang, J., Andreae, M. O., Barbosa, H. M. J., Fan, J., Fisch, G., Goldstein, A. H., Guenther, A., Jimenez, J. L., Pöschl, U., Silva Dias, M. A., Smith, J. N., and Wendisch, M.: Introduction: Observations and Modeling of the Green Ocean Amazon (GoAmazon2014/5), *Atmos. Chem. Phys.*, 16, 4785-4797, [10.5194/acp-16-4785-2016](https://doi.org/10.5194/acp-16-4785-2016), 2016.
- Martin, S. T., Artaxo, P., Machado, L., Manzi, A. O., Souza, R. A. F., Schumacher, C., Wang, J., Biscaro, T., Brito, J., Calheiros, A., Jardine, K., Medeiros, A., Portela, B., Sá, S. S. d., Adachi, K., Aiken, A. C., Albrecht, R., Alexander, L., Andreae, M. O., Barbosa, H. M. J., Buseck, P., Chand, D., Comstock, J. M., Day, D. A., Dubey, M., Fan, J., Fast, J., Fisch, G., Fortner, E., Giangrande, S., Gilles, M., Goldstein, A. H., Guenther, A., Hubbe, J., Jensen, M., Jimenez, J. L., Keutsch, F. N., Kim, S., Kuang, C., Laskin, A., McKinney, K., Mei, F., Miller, M., Nascimento, R., Pauliquevis, T., Pekour, M., Peres, J., Petäjä, T., Pöhlker, C., Pöschl, U., Rizzo, L., Schmid, B., Shilling, J. E., Dias, M. A. S., Smith, J. N., Tomlinson, J. M., Tóta, J., and Wendisch, M.: The Green Ocean Amazon Experiment (GoAmazon2014/5) Observes Pollution Affecting Gases, Aerosols, Clouds, and Rainfall over the Rain Forest, *Bull. Am. Meteorol. Soc.*, 98, 981-997, [10.1175/bams-d-15-00221.1](https://doi.org/10.1175/bams-d-15-00221.1), 2017.
- Medeiros, A. S. S., Calderaro, G., Guimarães, P. C., Magalhaes, M. R., Morais, M. V. B., Rafee, S. A. A., Ribeiro, I. O., Andreoli, R. V., Martins, J. A., Martins, L. D., Martin, S. T., and Souza, R. A. F.: Power plant fuel switching and air quality in a tropical, forested environment, *Atmos. Chem. Phys.*, 17, 8987-8998, [10.5194/acp-17-8987-2017](https://doi.org/10.5194/acp-17-8987-2017), 2017.



- Misenis, C., and Zhang, Y.: An examination of sensitivity of WRF/Chem predictions to physical parameterizations, horizontal grid spacing, and nesting options, *Atmos. Res.*, **97**, 315-334, 10.1016/j.atmosres.2010.04.005, 2010.
- Mlawer, E. J., Taubman, S. J., Brown, P. D., Iacono, M. J., and Clough, S. A.: Radiative transfer for inhomogeneous atmospheres: RRTM, a validated correlated-k model for the longwave, *J. Geophys. Res.*, **102**, n. D14, 16663-16682, 10.1029/97JD00237, 1997.
- Oliveira, A. P., and Fitzjarrald, D. R.: The Amazon river breeze and the local boundary layer: I. Observations, *Bound.-Layer Meteorol.*, **63**, 141-162, 10.1007/BF00705380, 1993.
- Oliveira, A. P., and Fitzjarrald, D. R.: The Amazon river breeze and the local boundary layer: II. Linear analysis and modelling, *Bound.-Layer Meteorol.*, **67**, 75-96, 10.1007/BF00705508, 1994.
- Rafee, S. A. A., Martins, L. D., Kawashima, A. B., Almeida, D. S., Morais, M. V., Souza, R. V., Oliveira, M. B., Souza, R. A., Medeiros, A. S., and Urbina, V.: Contributions of mobile, stationary and biogenic sources to air pollution in the Amazon rainforest: a numerical study with the WRF-Chem model, *Atmos. Chem. Phys.*, **17**, 7977-7995, 10.5194/acp-17-7977-2017, 2017.
- Saha, S., Moorthi, S., Wu, X., Wang, J., Nadiga, S., Tripp, P., Behringer, D., Hou, Y.-T., Chuang, H.-y., Iredell, M., Ek, M., Meng, J., Yang, R., Mendez, M. P., van den Dool, H., Zhang, Q., Wang, W., Chen, M., and Becker, E.: NCEP Climate Forecast System Version 2 (CFSv2) 6-hourly Products, in: Research Data Archive at the National Center for Atmospheric Research, Computational and Information Systems Laboratory, Boulder, CO, 2011.
- Schmid, B., Tomlinson, J. M., Hubbe, J. M., Comstock, J. M., Mei, F., Chand, D., Pekour, M. S., Kluzek, C. D., Andrews, E., Biraud, S. C., and McFarquhar, G. M.: The DOE ARM Aerial Facility, *Bull. Am. Meteorol. Soc.*, **95**, 723-742, 10.1175/bams-d-13-00040.1, 2014.
- Sioli, H.: The Amazon and its main affluents: hydrography, morphology of the river courses, and river types, in: *The Amazon*, Springer, 127-165, 1984.
- Trebs, I., Mayol-Bracero, O. L., Pauliquevis, T., Kuhn, U., Sander, R., Ganzeveld, L., Meixner, F. X., Kesselmeier, J., Artaxo, P., and Andreae, M. O.: Impact of the Manaus urban plume



on trace gas mixing ratios near the surface in the Amazon Basin: Implications for the NO-NO₂-O₃ photostationary state and peroxy radical levels, *J. Geophys. Res.*, 117, n. D5, 10.1029/2011JD016386, 2012.

Ying, Z., Tie, X., and Li, G.: Sensitivity of ozone concentrations to diurnal variations of surface emissions in Mexico City: A WRF/Chem modeling study, *Atmos. Environ.*, 43, 851-859, 10.1016/j.atmosenv.2008.10.044, 2009.



List of Figures

Figure 1. Satellite image of the Manaus region. The Rio Negro comes from the northwest, and the Rio Solimões arrives from the west. The confluence of the two rivers is to the southeast of Manaus, beginning the Amazon River (“Rio Amazonas”). Yellow markers show locations of (i) the measurement supersite called “T3”, (ii) two river locations “R1” and “R2” considered in the modeling methodology herein, and (iii) points “A”, “B”, and “C” along a river cross section, also used in the methodology herein.

Figure 2. Mean horizontal wind speeds for March 2014. The left column represents the base case wR (“with rivers”). The right column represents the difference case (wR - woR) (“with rivers compared to without rivers”). Rows represent altitude as (1) near surface, (2) 100 m, and (3) 500 m.

Figure 3. Difference in mean horizontal wind speed for (wR - woR) (“with rivers compared to without rivers”). Plots are shown as vertical cross sections along points A, B, and C of the Figure 1 as follows: (a) for all of March 2014, (b) at 00:00, (c) at 06:00, (d) at 12:00, and (e) at 18:00, all in local time (UTC - 4 h).

Figure 4. Concentrations of O₃, NO_x, and CO measured by instrumentation on board an aircraft during GoAmazon2014/5 at an altitude of approximately 500 m (Martin et al., 2017). Concentrations are plotted in false color, and the legends on the right-hand side of each row show the scaling. Below each main panel, a line plot shows the concentrations marked by points A through H along the flight paths. Red shading demarcates periods when the aircraft was flying over a river.

Figure 5. Time series of O₃ concentrations at the T3, R1, and R2 locations. The left column plots



the cases of wR (“with rivers”; blue) and woR (“without rivers”; red). The right column shows the difference in concentrations as (wR - woR).

Figure 6. Time series of NO_x concentrations at the T3, R1, and R2 locations. The left column plots the cases of wR (“with rivers”; blue) and woR (“without rivers”; red). The right column shows the difference in concentrations as (wR - woR).

Figure 7. Time series of CO concentrations at the T3, R1, and R2 locations. The left column plots the cases of wR (“with rivers”; blue) and woR (“without rivers”; red). The right column shows the difference in concentrations as (wR - woR).

Figure 8. Near-surface concentrations of (a) O₃, (b) NO_x, and (c) CO (March 2, 13:00 local time, UTC - 4 h). The first and second columns represent the cases of wR (“with rivers”) and woR (“without rivers”), respectively. The vector field in each panel shows the near-surface horizontal winds. The third column shows the difference in concentrations as (wR - woR). For reference, the locations of T3, R1, and R2 are marked.

**Table 1.** Percent change in pollutant concentration X for the case of wR (“with rivers”)

compared to that of woR (“without rivers”), calculated as $(X_{wR} - X_{woR})/X_{woR}$, where X is the monthly mean at a location T3, R1, or R2 for each of O₃, NO_x, and CO.

	O ₃	NO _x	CO
T3	+5.5%	-4.6%	+1.2%
R1	+28.4%	+26.0%	+2.9%
R2	+25.5%	+25.6%	+2.6%

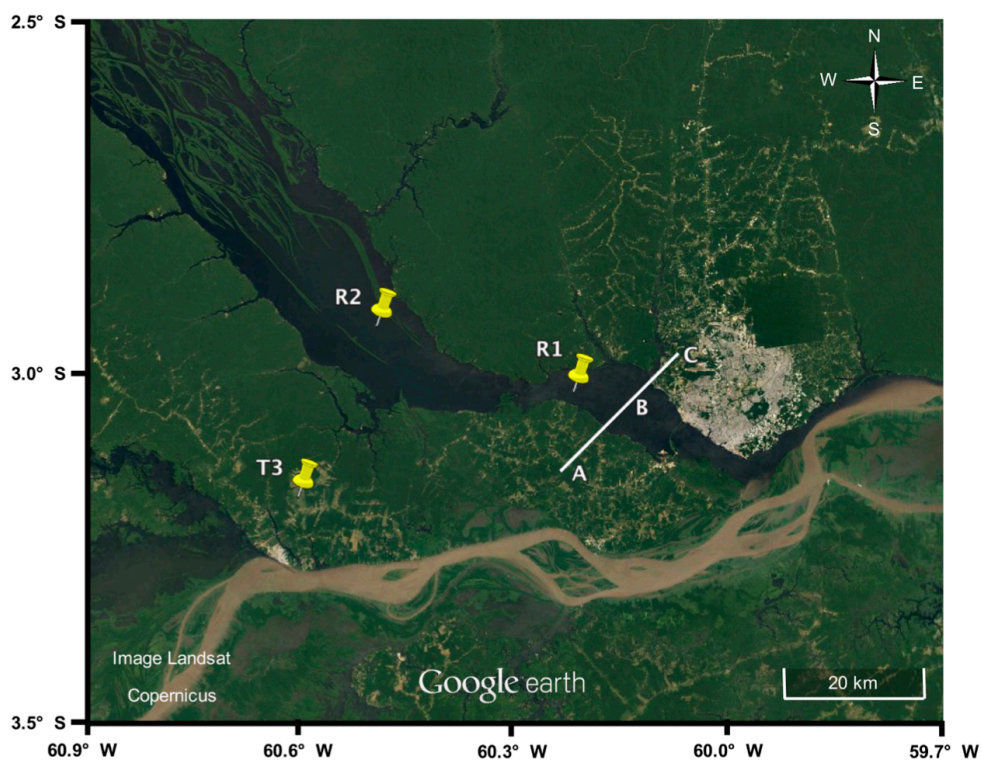


Figure 1

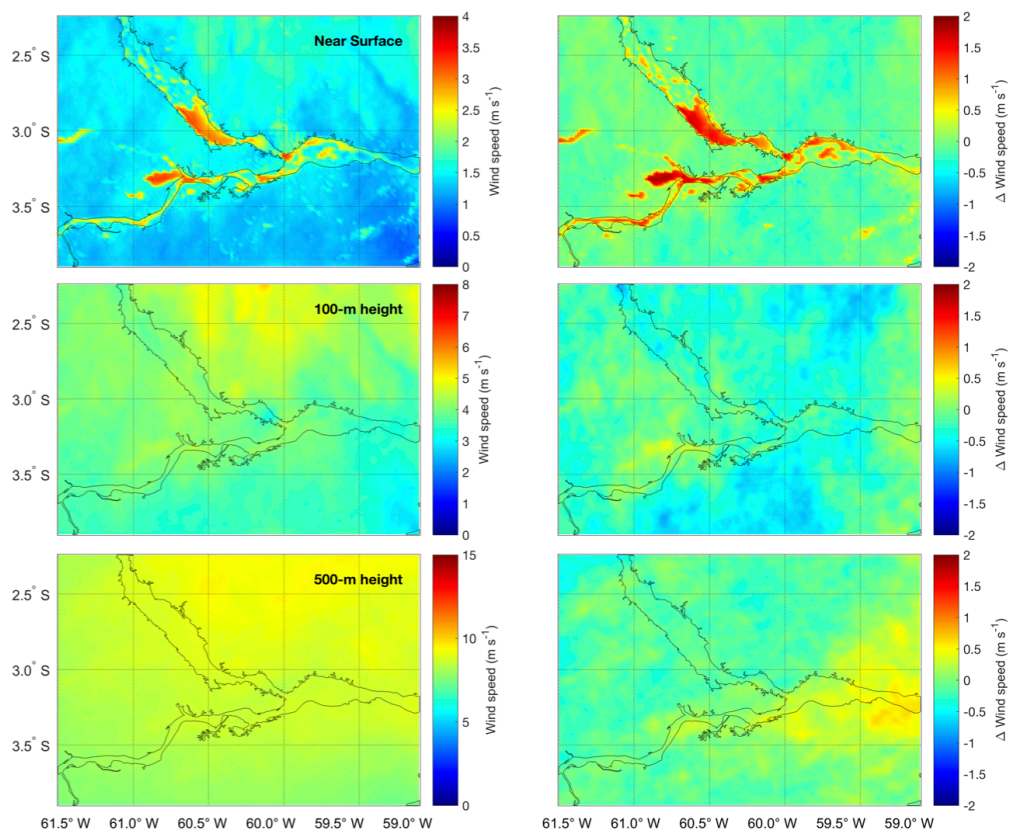


Figure 2

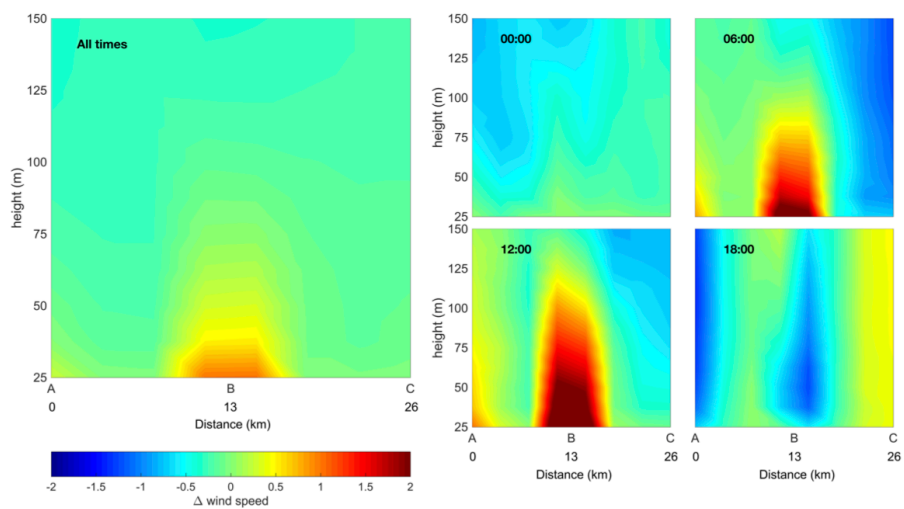


Figure 3

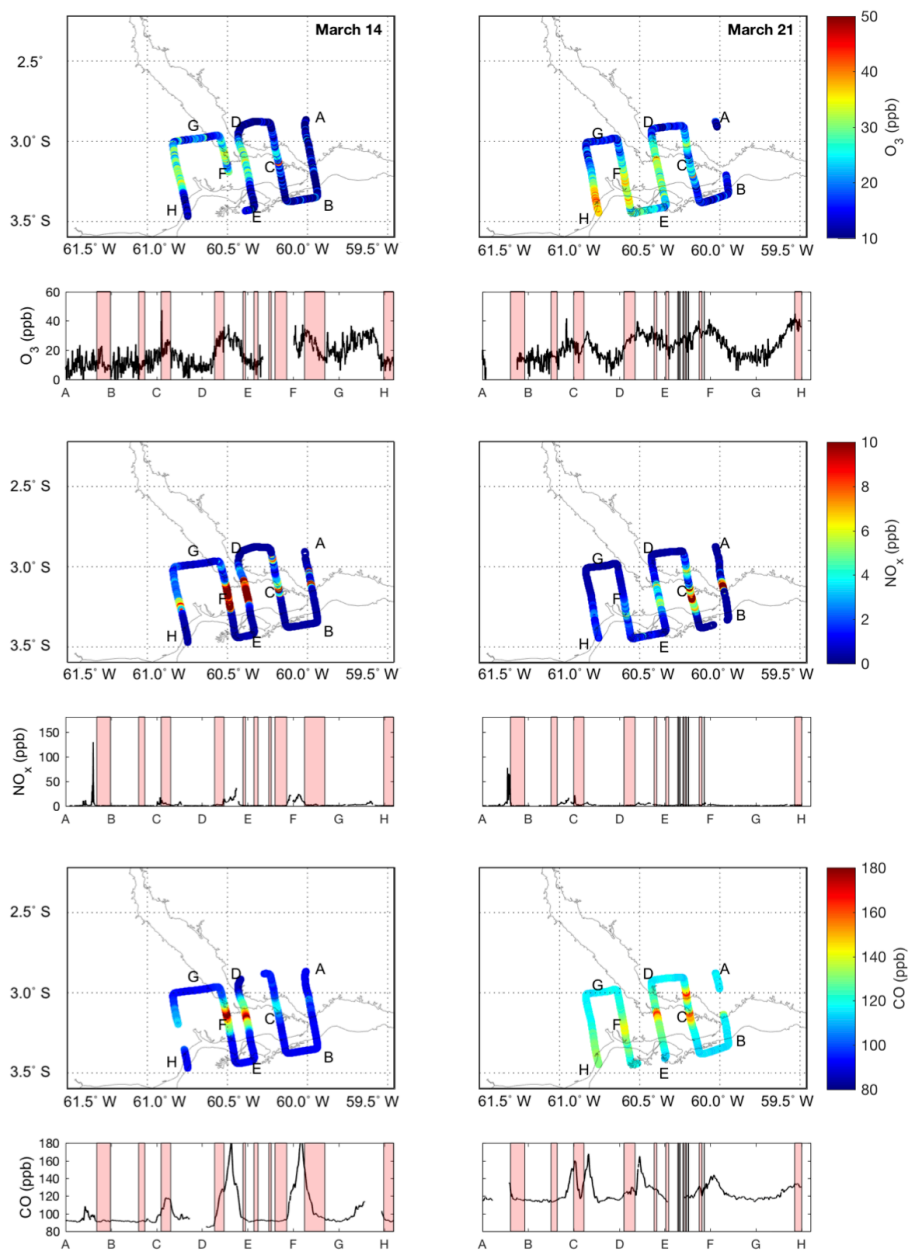


Figure 4

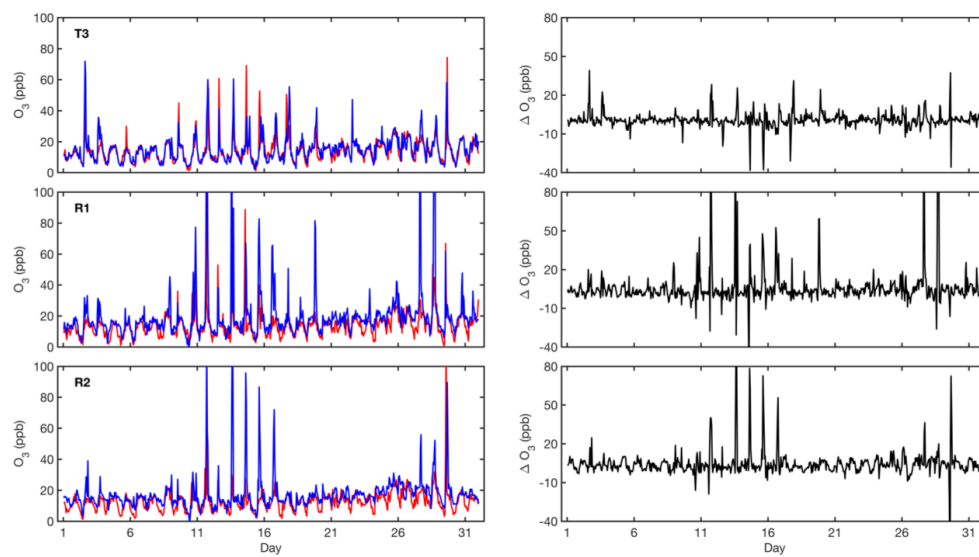


Figure 5

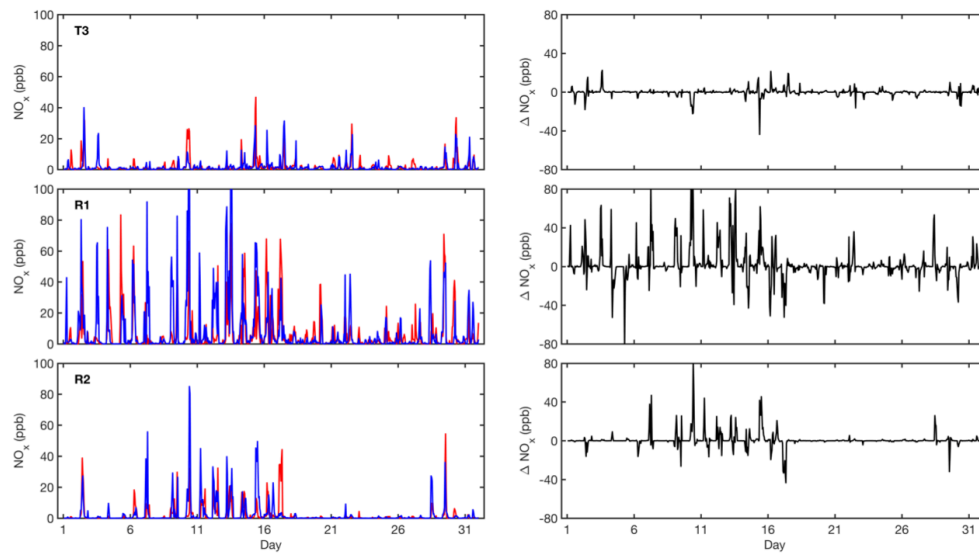


Figure 6

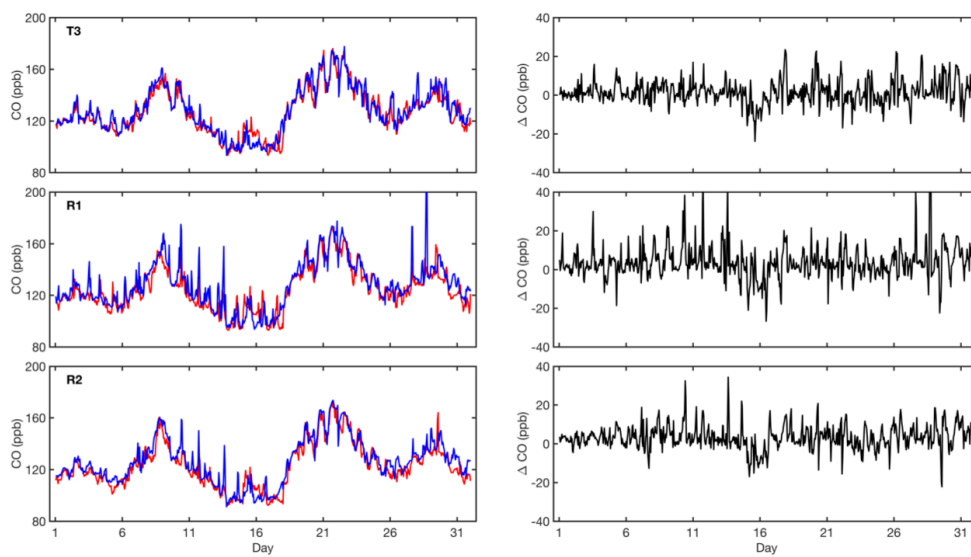


Figure 7

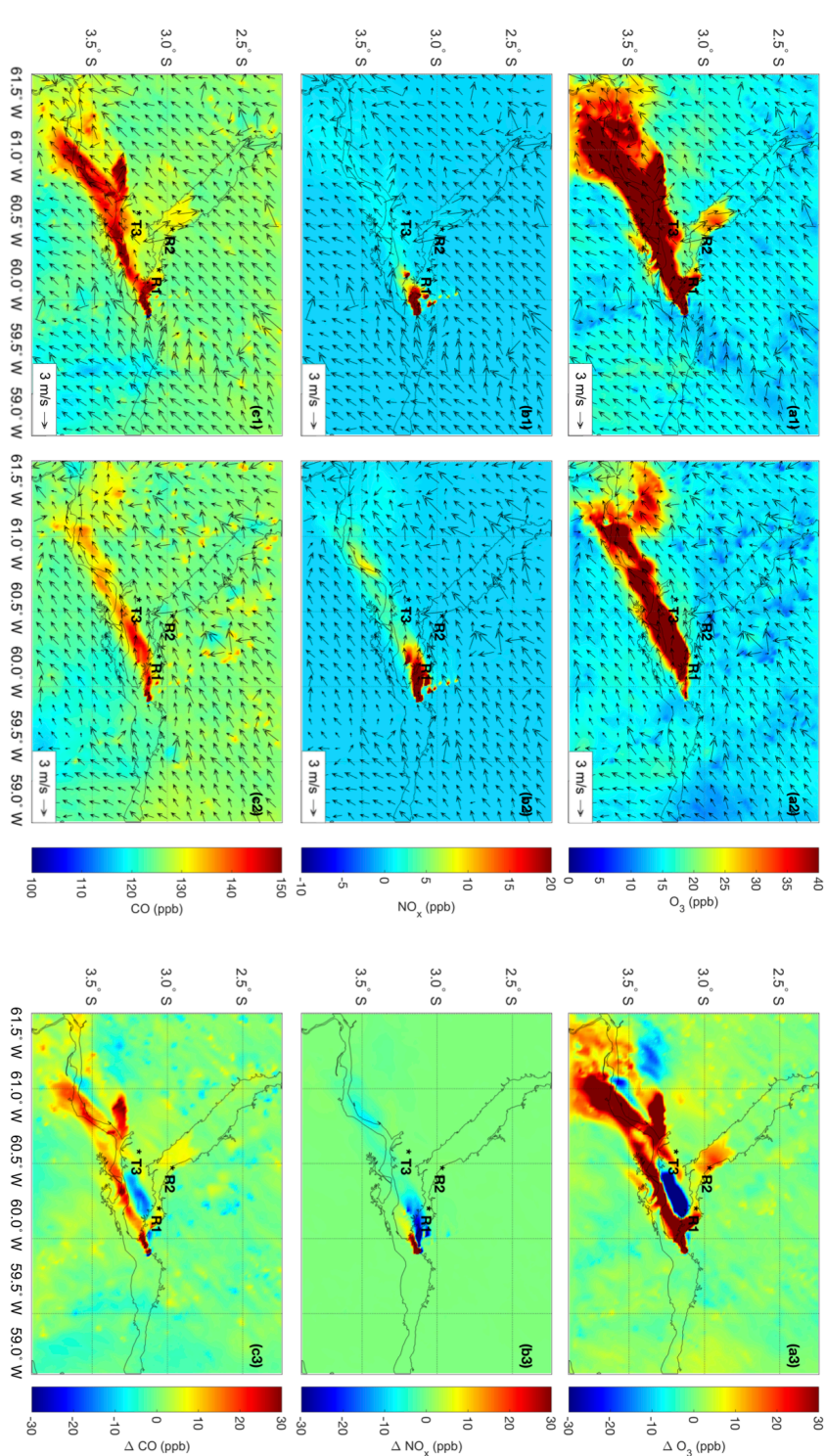


Figure 8